Journal of Coordination Chemistry
Publication details, including instructions for authors and subscription information:
http://www.tandfonline.com/loi/gcoo20

Keggin-type cesium salt of first series transition metal-substituted phosphomolybdates: one-pot easy synthesis, structural, and spectral analysis

Anjali Patel [a] & Soyeb Pathan [a]
[a] Department of Chemistry, Faculty of Science , M. S. University of Baroda , Vadodara - 390002 , Gujarat , India
Accepted author version posted online: 10 Jul 2012.Published online: 27 Jul 2012.

To cite this article: Anjali Patel & Soyeb Pathan (2012) Keggin-type cesium salt of first series transition metal-substituted phosphomolybdates: one-pot easy synthesis, structural, and spectral analysis, Journal of Coordination Chemistry, 65:17, 3122-3132, DOI: 10.1080/00958972.2012.710843

To link to this article: http://dx.doi.org/10.1080/00958972.2012.710843

Journal of Coordination Chemistry
Vol. 65, No. 17, 10 September 2012, 3122–3132

Keggin-type cesium salt of first series transition metal-substituted phosphomolybdates: one-pot easy synthesis, structural, and spectral analysis

ANJALI PATEL* and SOYEB PATHAN

Department of Chemistry, Faculty of Science, M. S. University of Baroda, Vadodara – 390002, Gujarat, India

(*Received 8 March 2012; in final form 8 July 2012*)

The Keggin-type cesium salt of transition metal-substituted phosphomolybdates, $Cs_5[PCo(H_2O)Mo_{11}O_{39}]\cdot 6H_2O$ (**1**) and $Cs_5[PMn(H_2O)Mo_{11}O_{39}]\cdot 6H_2O$ (**2**), were synthesized from commercially available $H_3PMo_{12}O_{40}$. The compounds were characterized by thermal, structural, and spectroscopic techniques. X-ray structural analysis reveals that, in these isostructural disordered compounds, the transition metal (Co/Mn) and Mo atoms are distributed over 12 positions. The presence of Co/Mn atoms was confirmed by powder XRD, FT-IR, DR-UV-Vis, ESR, and ^{31}P NMR studies.

Keywords: Keggin; Polyoxometalates; Substituted phosphomolybdate; Cobalt; Manganese

1. Introduction

Keggin-type polyoxometalates (POMs) are a rich class of inorganic metal-oxide cluster compounds with transition metals in their highest oxidation states and have a general formula $[X^{n+}M_{12}O_{40}]^{(8-n)-}$, where X^{n+} is a central heteroatom (Si^{4+}, P^{5+}, etc.) and M are addenda atom (W^{6+}, Mo^{6+}, V^{5+}, etc.) [1–3]. They possess structural variety and interesting properties for potential applications in catalysis, materials science, and medicine [1, 2]. A subclass of Keggin-type POMs, transition metal-substituted POMs (TMSPs), $[XM_{11}M'O_{39}]^{(n-m)-}$ (X = P, Si, B; M = W, Mo; M′ = transition metal), have received increasing attention because substitution of a transition metal into the POM has been explored as a route to increase the range of application of these compounds [4–7]. TMSPs are useful single-site catalysts where the active metal M is isolated in, and strongly bound to, an inorganic metal-oxide matrix and thus is prevented from oligomerization and leaching [8, 9].

Among the various Keggin-type TMSPs, cobalt-substituted POMs and manganese-substituted POMs are of interest for their variable oxidation states and redox properties [4]. A literature survey shows several reports on the synthesis and characterization of cobalt/manganese-substituted polyoxotungstates [10–18] as well as

*Corresponding author. Email: aupatel_chem@yahoo.com

ISSN 0095-8972 print/ISSN 1029-0389 online
http://dx.doi.org/10.1080/00958972.2012.710843

silicotungstates [10, 19–21]. At the same time, reports on analogous compounds based on phosphomolybdates are limited.

Combs-Walker and Hill reported a two-step synthesis of tetrabutyl ammonium salt of transition metal-substituted phosphomolybdates (M = Co, Mn, Cu, and Zn) [22]. Lin *et al.* reported a chain-like crystal structure of $[(CH_3)_3NH]_{5n}[PMo_{11}MO_{39}]^n \cdot xH_2O$ ($M = Mn^{2+}$, $x = n$; Co^{2+}, $x = 2n$) [23]. This method involves synthesis from the individual transition metal salts (i.e., $Na_2MoO_4 \cdot 2H_2O$ and $Co(CH_3COO)_2$). They investigated electrochemical and magnetic properties of these compounds. Rabia *et al.* reported the synthesis of the ammonium salt of cobalt substituted from individual transition metal salts (ammonium heptamolybdate, cobalt sulfate) [24].

The syntheses, crystal structures, and physical properties of a series of radical salts made with bis(ethylenedithio)tetrathiafulvalene (BEDT-TTF or ET) and mono Mn-substituted Keggin phosphomolybdate of formula $[PMn(H_2O)Mo_{11}O_{39}]^{5-}$ have been reported by Coronado *et al.* [25]. Hu and Burns synthesized and characterized a series of transition metal-substituted phosphomolybdates $(Na_2[(C_4H_9)_4N]_4[PZ(II)(Br)Mo_{11}O_{39}]$, where Z = Mn(II), Co(II), Ni(II), Cu(II), and Zn(II)) [26].

These reported articles describe syntheses of the Co(II)/Mn(II)-substituted phosphomolybdates either in two steps [24] or from the individual transition metal salts [23–26]. Except two reports [23, 25], authors have not reported any crystal structure. No reports describing discrete Keggin structures for the cesium salt of Co(II)/Mn(II)-substituted phosphomolybdate is available. It was thought of interest to develop an easy one-step method for the synthesis of cesium salts of Co(II)/Mn(II)-substituted phosphomolybdate as well as detailed characterization including single-crystal XRD.

In this article, we report one-pot synthesis of the cesium salt of mono transition metal-substituted phosphomolybdate from commercially available 12-molybdophosphoric acid and acetates of the transition metals (Co, Mn). The synthesized compounds were characterized by single-crystal X-ray diffraction, powder X-ray diffraction, elemental analysis, TG-DTA, FT-IR, diffused reflectance spectra (DRS), electron spin resonance (ESR), and ^{31}P MAS NMR. As an application, a preliminary study was carried out to explore the use of synthesized compounds for the oxidation of styrene.

2. Experimental

2.1. *Materials*

All chemicals used were of A.R. grade. 12-Molybdophosphoric acid, $H_3PMo_{12}O_{40}$, $NaHCO_3$, CsCl, $Co(CH_3COO)_2 \cdot 4H_2O$, and $Mn(CH_3COO)_2 \cdot 4H_2O$ were obtained from Merck and used as received.

2.2. *Synthesis of Co(II)-substituted phosphomolybdate (1)*

Co(II)-substituted phosphomolybdate (**1**) was synthesized using the following procedure. The pH of a solution of $H_3PMo_{12}O_{40}$ (1.825 g, 1 mmol) in water (5 mL) was adjusted to 4.3 using $NaHCO_3$. The solution was heated to 80°C by stirring. A solution of cobalt acetate (0.249 g, 1 mmol) in water (5 mL) was added

to this hot solution. The final pH of the solution was 4.3. The solution was heated at 80°C by stirring for 1 h and filtered hot. A saturated solution of CsCl was added to the hot filtrate. The resulting mixture was allowed to stand overnight at room temperature. The obtained dark reddish brown X-ray quality crystals (yield 60%) were filtered and air dried. The filtrate was used for the estimation of molybdenum and cobalt.

2.3. *Synthesis of Mn(II)-substituted phosphomolybdate (2)*

The same procedure was followed for the synthesis of Mn(II)-substituted phosphomolybdate (**2**). Instead of cobalt acetate, 0.245 gm of Mn-acetate was added. Dark brown X-ray quality crystals (yield 58%) were obtained. The filtrate was used for the estimation of molybdenum and manganese.

2.4. *Characterization*

2.4.1. X-ray crystallography. Single-crystal X-ray data were collected at 298 K on a BRUKER SMART APEX CCD area detector system with [λ (Mo-K$\alpha = 0.71073$ Å)] a graphite monochromator. Two thousand frames were recorded with an ω scan width of 0.3°, each for 10 s, crystal detector distance 60 mm, collimator 0.5 mm. The data were reduced using SAINTPLUS [27] and a multi-scan absorption correction using SADABS [27] was performed. Structure solution and refinement were done using SHELX-97 [28]. All non-hydrogen atoms were refined anisotropically. Details of the crystal data are presented in table 1.

2.4.2. Analytical techniques. The XRD pattern was obtained using PHILIPS PW-1830. The conditions were: Cu-Kα radiation (1.54 Å), scanning angle from 0° to 80°. The filtrate was analyzed for molybdenum gravimetrically, and cobalt and manganese volumetrically [29]. Elemental analysis was carried out using the JSM 5610 LV EDX-SEM analyzer. TG-DTA was carried out on a Mettler Toledo Star SW 7.01 up to 600°C in air with a heating rate of 5°C min^{-1}. FT-IR spectra of the sample were obtained using a KBr wafer on the Perkin Elmer instrument. The DRUV-Visible spectrum was recorded at room temperature on a Perkin Elmer LAMBDA instrument using a 1 cm quartz cell. ESR spectra were recorded on a Varian E-line Century series X-band ESR spectrometer (room temperature and scanned from 2000 to 3200 Gauss). ^{31}P MAS NMR spectra were recorded on a Bruker Avance DSX-300 NMR spectrometer at 121.48 MHz using a 7 mm rotor probe with 85% phosphoric acid as an external standard. The spinning rate was 4–5 kHz.

3. Results and discussion

Compounds **1** and **2** were isolated as the cesium salts after completion of the reaction and the remaining solution was filtered. The filtrate was analyzed for molybdenum

Table 1. Crystal data and collection parameters for **1** and **2**.

	1	**2**
Empirical formula	$Cs_5Mo_{11}CoO_{46}P$	$Cs_5Mo_{11}MnO_{46}P$
Formula weight	2559.74	2555.74
Crystal system	Tetragonal	Tetragonal
Space group	*P42/ncm*	*P42/ncm*
Unit cell dimensions (Å, °)		
$a = b$	20.7451(12)	20.7353(8)
c	10.3976(13)	10.3479(8)
$\alpha = \beta = \gamma$	90	90
Temperature (K)	293(2)	110(2)
Volume (Å^3), Z	4474.7(7), 4	4449.1(4), 4
Calculated density (Mg m^{-3})	4.031	4.054
Absorption coefficient (mm^{-1})	8.205	8.252
$F(000)$	4868	4868
Crystal size (mm^3)	$0.45 \times 0.20 \times 0.08$	$0.24 \times 0.12 \times 0.04$
θ range for data collection (°)	2.40–27.73	1.96–27.49
Reflections collected/unique	20,941	21,013
Independent reflection	2057 [R(int) = 0.0280]	2652 [R(int) = 0.0294]
Max. and min. transmission	0.5598 and 0.1196	0.7337 and 0.2421
Refinement method	Full-matrix least-squares on F^2	Full-matrix least-squares on F^2
Data/restraints/parameters	2057/0/164	2652/0/162
Goodness-of-fit on F^2	1.322	1.214
Final R indices [$I > 2\sigma(I)$]	$R_1 = 0.0967$, $wR_2 = 0.1942$	$R_1 = 0.0688$, $wR_2 = 0.1892$
R indices (all data)	$R_1 = 0.0948$, $wR_2 = 0.1931$	$R_1 = 0.0695$, $R_2 = 0.1897$

gravimetrically, and cobalt and manganese volumetrically [29]. The observed proportion of Mo in the filtrate was 0.5%, which corresponds to the loss of one equivalent of Mo from $H_3PMo_{12}O_{40}$. The proportions Co and Mn in the filtrates were 0.0235% and 0.0231%, corresponding to the incorporation of one equivalent of cobalt and manganese into the lacunary species created by the removal of one Mo.

Observed EDX values for the elemental analysis of the isolated compounds were in good agreement with the theoretical values.

For **1**: Anal. Calcd (%): Cs, 25.88; Mo, 41.20; P, 1.20; Co, 2.30; O, 28.75. Found (%): Cs, 25.90; Mo, 41.29; P, 1.16; Co, 2.33; O, 28.69.

For **2**: Anal. Calcd (%): Cs, 26.00; Mo, 41.29; P, 1.21; Mn, 2.15; O, 28.79. Found (%): Cs, 26.34; Mo, 41.40; P, 1.18; Mn, 2.04; O, 28.61.

3.1. *Crystal structure and thermal analysis*

Crystal structure analysis of both the compounds shows that cobalt and manganese are not present as counter cations; Cs is the counter cation with Cs–P distances of 8.338 and 10.517 Å. The crystallographic refinement of **1** and **2** suggests the presence of 5.44 and 6 Cs per Keggin unit as counter ions, while the elemental analysis confirms the presence of 5 Cs atoms for each polyanion. Due to the large difference in the electron densities of H and Mo, the presence of H could not be confirmed from the structural data. The proportion of H_2O was calculated from the TGA curve (Supplementary material); the total observed weight loss (4.83%) at 150°C corresponds to the loss of seven water molecules for both the compounds. Similarly, DTA of both the compounds showed an

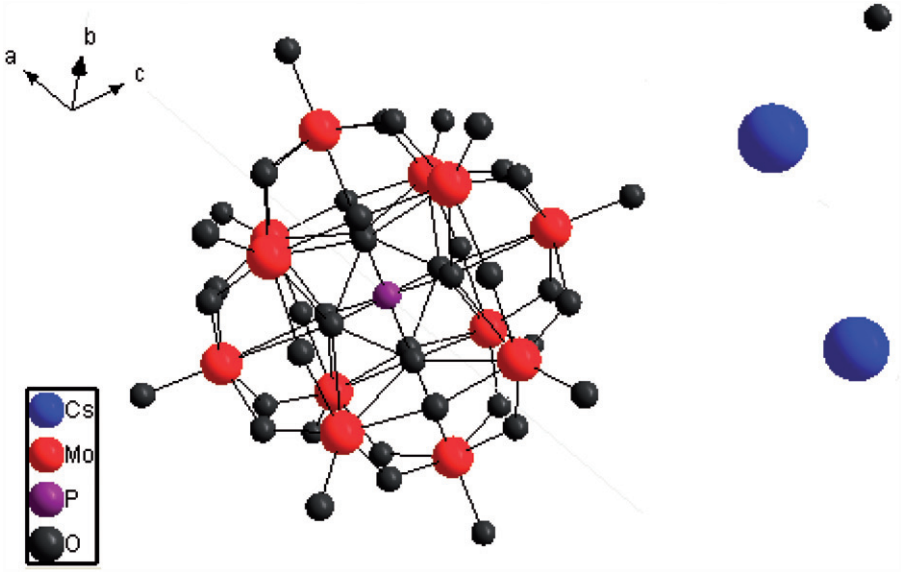

Figure 1. Disordered Keggin-type structure.

endothermic peak from 60°C to 150°C due to the water molecule of crystallization. Exothermic peaks at 360°C and 415–430°C were observed due to the decomposition of the Keggin unit and the formation of corresponding metal oxides. Thus, based on the structural, elemental analysis, and thermal analysis, the formulas of the compounds are proposed as $Cs_5[PCo(H_2O)Mo_{11}O_{39}] \cdot 6H_2O$ and $Cs_5[PMn(H_2O)Mo_{11}O_{39}] \cdot 6H_2O$.

The compounds show two types of disorder in the crystal; figure 1 shows the disordered Keggin-type structure. In **1**, Co was distributed over the 12 positions and Co could not be distinguished from the 11 Mo's distributed equally over the 12 addenda atoms in the Keggin structure. The Keggin polyanion is also distributed over two orientations related by a center of symmetry [30–32]. Similar disorder is observed for **2**.

The packing structure of both the complexes indicates that cesium atoms occupy voids created due to close packing (figure 2). Water molecules are also expected to be present in the voids and are interconnected *via* weak H-bonds. During the final refinement cycle, isotropic thermal parameters for oxygen indicated the presence of different oxygen atoms than of the Keggin unit; these originate from the adsorbed water.

The typical Keggin structure has three different types of Mo–O bond distances, O-terminal (1.70 Å), O-*cis* bridging (1.90 Å), and O-*trans* bridging (2.46 Å). In Keggin-type POMs, the central tetrahedral PO_4 is surrounded by twelve MoO_6 octahedra in four groups of Mo_3O_{13} units. If the structure is totally symmetrical, PO_4 has a T_d symmetry with all P–O bond lengths in the range of 1.51–1.55 Å.

In **1**, the central four oxygen atoms (bonded to three Mo and one P) are disordered over eight positions, from which three different types of P–O bonds are obtained. Three of these have almost the same bond length of 1.502 and 1.533 Å while the fourth P–O bond has a longer length of 1.615 Å (O12), indicating distortion in PO_4 symmetry. This may be due to the change in the environment around the corresponding Mo_3O_{13} unit.

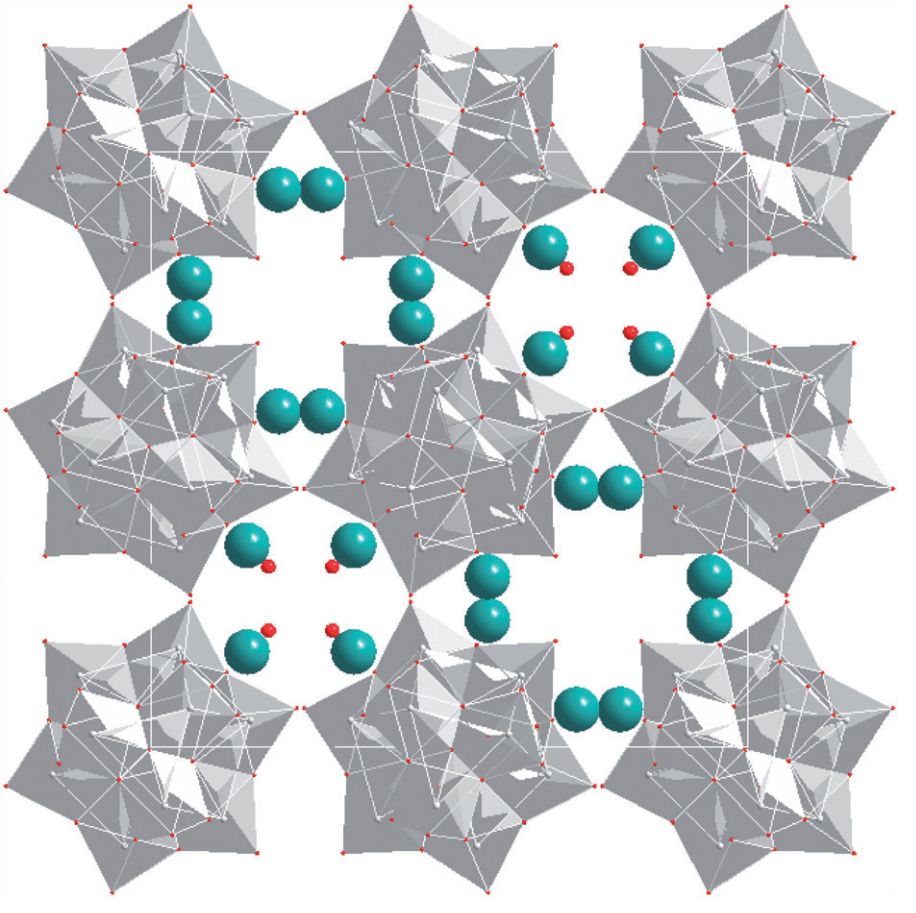

Figure 2. Packing diagram.

Hence, the change in the environment due to the substitution of Co in the corresponding Mo_3O_{13} and P–O12–Mo_3O_{13} moieties is as expected. Mo2, Mo2, and Mo4 are attached to O12. The Mo4–O12 bond length is 2.48 Å. The corresponding terminal oxygen attached to Mo4 is O14. As mentioned earlier, the presence of disorder in the crystal structure is at O14, and hence, the probability of Co substitution is maximum at Mo4. Similarly, in **2**, three different types of P–O bonds are obtained for four P–O bonds. Three of these have almost equal bond length of 1.527 and 1.557 Å while the fourth P–O bond has a longer length of 1.619 Å (O13), indicating distortion in PO_4 symmetry. The change in the environment due to the substitution of Mn in the corresponding Mo_3O_{13} and P–O13–Mo_3O_{13} moieties is as expected. The three Mo's attached to O13 are Mo1, Mo1, and Mo4. The Mo4–O13 bond length is 2.493 Å. The corresponding terminal oxygen attached to Mo4 is O10. The presence of disorder in the crystal structure is at O10, and hence, the probability of Mn substitution is maximum at Mo4.

Cs cations show a number of contacts with the anions and extensive cooperation between cations throughout the crystal is important to form a continuous network that stabilizes the structure and makes the crystals stable in air.

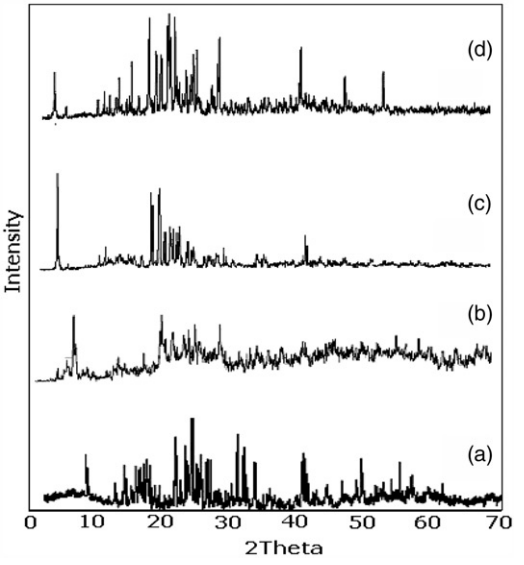

Figure 3. Powder X-ray pattern of (a) PMo_{12}, (b) PMo_{11}, (c) **1**, and (d) **2**.

The powder XRD patterns of **1** and **2** along with the simulated patterns using the data set obtained by the single-crystal analysis are presented in the ''Supplementary material.'' The experimental and simulated patterns are similar, indicating that the single-crystal and bulk structures are identical.

The XRD patterns of **1** and **2** are totally different from $[PMo_{12}O_{40}]^{3-}$ (PMo_{12}) while it resembled $[PMo_{11}O_{39}]^{7-}$ (PMo_{11}), confirming the presence of 11Mo in the synthesized compounds. Along with the characteristic peak of PMo_{11}, additional peaks were found for **1** and **2** due to the incorporation of transition metal into the lacunary position of phosphomolybdate (figure 3c and d).

3.2. *FTIR analysis*

The frequencies of FT-IR bands for PMo_{12}, **1,** and **2** are shown in the ''Supplementary material.'' The FT-IR of PMo_{12} showed bands at 1070, 965, and 870 and 790 corresponding to the symmetric stretching of P–O, Mo–O, and Mo–O–Mo bonds, respectively. The FT-IR showed the P–O bond frequencies of 1050 and 1043 cm^{-1} for **1** and **2**, respectively. The shift in the band position compared to PMo_{12} indicates that Mn(II) was introduced into the octahedral lacuna. There is also a shift in the stretching vibration of Mo=O and Mo–O–Mo for both the compounds, indicating complexation of the transition metals. An additional band at 480 and 422 cm^{-1} is attributed to the Co–O and Mn–O vibrations, respectively. Thus, the FT-IR spectra clearly show the incorporation of Co/Mn into the Keggin framework and not present as a counter cation since no appreciable shifting would be expected in this case.

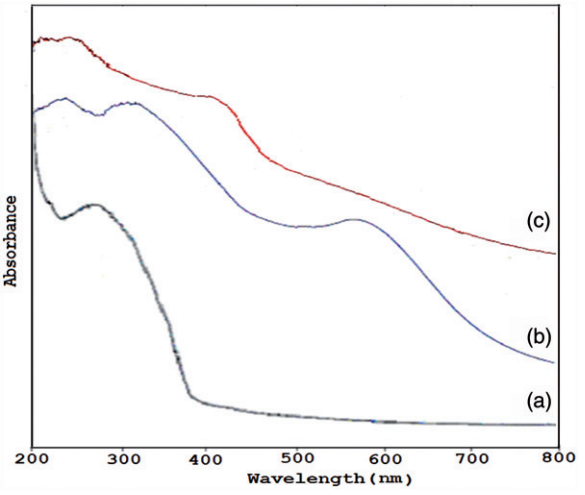

Figure 4. DRS of (a) PMo_{11}, (b) **1**, and (c) **2**.

3.3. *Diffused reflectance spectra*

Figure 4 shows the DRS for PMo_{11}, **1**, and **2**. For PMo_{11}, intense absorption bands at ~285 nm are caused due to $O \rightarrow Mo$ charge transfer. The DRS of **1** and **2** show two peaks. A peak at 270 nm corresponds to $O \rightarrow Mo$ charge transfer, indicating the formation of $PMo_{11}O_{39}$ lacuna in the synthesized compounds. The observed shift as compared to that of PMo_{11} may be due to the substitution of transition metal. The DRS of **1** and **2** show broad bands at 560–580 and 390–430 nm due to the presence of Co(II) and Mn(II) in the compounds, respectively.

3.4. *Electron spin resonance*

The presence of Co(II) and Mn(II) in **1** and **2** was confirmed by ESR. The full range (3200–2000 G) X-band room temperature ESR spectra (figure 5) for both the compounds were recorded. ESR spectra of **1** show eight hyperfine signals (Co^{2+}; $I = 7/2$), confirming presence of Co(II). The g value is ~2.66, which shows Co(II) is in an octahedral or a distorted octahedral environment.

Similarly, ESR spectra of **2** show six signals (Mn^{2+}; $s = 5/2$), indicating the presence of Mn(II) with an octahedral or a distorted octahedral symmetry. Mn(II) introduced into octahedral lacuna of the Keggin structure should have a g value of ~2 for an octahedral or a distorted octahedral environment [14], confirming the presence of Mn(II).

3.5. *^{31}P MAS NMR*

The effect of paramagnetic Co(II) and Mn(II) was reflected in ^{31}P MAS NMR, indicating the absence of the chemical shift of **1** and **2** [24].

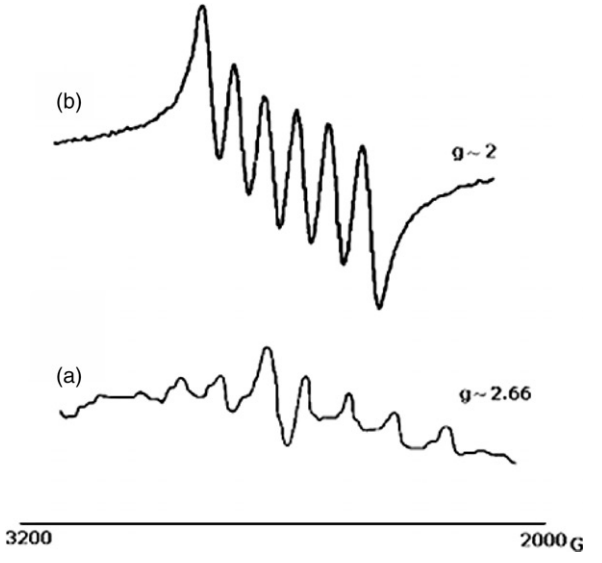

Figure 5. ESR spectra of (a) **1** and (b) **2**.

3.6. *Preliminary study on oxidation of styrene using hydrogen peroxide*

A preliminary study was carried out to evaluate the catalytic activity of **1** and **2** for oxidation. Oxidation of styrene (10 mmol) with aqueous H_2O_2 (30 mmol) was carried out in a glass reactor with a double-walled condenser containing 20 mg catalyst at 80°C with constant stirring for 10 h. After completion of the reaction, catalyst was removed and the product was extracted with dichloromethane. The product was dried with magnesium sulfate and analyzed by gas chromatography using a BP-5 capillary column. Product was identified by comparing with the authentic samples and finally by gas chromatography–mass spectroscopy (GC–MS).

Compound **1** shows >99% conversion with 97% selectivity for benzaldehyde with 1264 turn over number (TON) and **2** shows 67% conversion with 98% selectivity for benzaldehyde with 856 TON. The results are outstanding in terms of percentage of conversion as well as percentage of selectivity for the desired product.

4. Conclusion

We have introduced a one-step synthesis and crystal structures of Keggin-type Cs-salts of mono cobalt- and manganese-substituted phosphomolybdates starting from the commercially available 12-molybdophosphoric acid. The presence of Co and Mn was confirmed by powder XRD, FT-IR, DR-UV-Vis, ESR, and ^{31}P NMR studies. The reported synthesis provides a new route to other transition metals, especially for first series transition metal-substituted phosphomolybdates. The synthesized compounds were used as catalysts for solvent-free, liquid-phase oxidation of styrene with H_2O_2. The superiority of the present catalysts lies in obtaining high conversion of styrene,

selectivity toward benzaldehyde as well as high TON. Compound **1** shows >99% conversion with 97% selectivity for benzaldehyde with 1264 TON and **2** shows 67% conversion with 98% selectivity for benzaldehyde with 856 TON. The catalysts are not only selective for the oxidation of styrene, but also promising alternatives for traditional oxidation catalysts. Work is in progress to establish these compounds as catalysts for the oxidation of alkanes, alkenes, and alcohols. These studies will be useful for exploring applications of POM-based materials as third generation catalysts.

Supplementary material

Further details of the crystal structure determination can be obtained from CSD 422216 for **1**, CSD 423392 **2**, TG-DTA, and simulated XRD.

Acknowledgments

One of the authors, Mr Soyeb Pathan, is thankful to UGC-MANF, New Delhi, for the financial support.

References

[1] M.T. Pope. *Heteropoly and Isopoly Oxometalates*, Springer-Verlag, Berlin (1983).
[2] M.T. Pope, A. Muller. *Angew. Chem. Int. Ed.*, **30**, 34 (1991).
[3] M.T. Pope, A. Muller. *Polyoxometalate Chemistry: From Topology via Self Assembly Applications*, Kluwer, Dordrecht (2001).
[4] C.L. Hill, R.B. Brown. *J. Am. Chem. Soc.*, **108**, 536 (1986).
[5] J.E. Toth, J.D. Melton, D. Cabelli, B.H.J. Bielski, F.C. Anson. *Inorg. Chem.*, **29**, 1952 (1990).
[6] C. Rong, F.C. Anson. *Inorg. Chem.*, **33**, 1064 (1994).
[7] A. Muller, L. Dloczik, E. Dittman, M.T. Pope. *Inorg. Chim. Acta*, **257**, 231 (1997).
[8] J.M. Thomas, R. Raja. *Top. Catal.*, **40**, 3 (2006).
[9] O.A. Kholdeeva. *Top. Catal.*, **40**, 229 (2006).
[10] C.M. Torne, G.F. Tourne, S.A. Malik, T.J.R. Weakly. *J. Inorg. Nucl. Chem.*, **32**, 3875 (1970).
[11] J.R. Galan-Mascaros, C. Gimenez-Saiz, S. Triki, C.J. Gomez-Garcia, E. Coronado, L. Ouahab. *Angew. Chem. Int. Ed. Engl.*, **34**, 1460 (1995).
[12] M. Sadakane, E. Steckhan. *J. Mol. Catal A: Chem.*, **114**, 221 (1996).
[13] J.R. Galan-Mascaros, C. Gimenez-Saiz, S. Triki, C.J. Gomez-Garcia, E. Coronado. *J. Am. Chem. Soc.*, **120**, 4671 (1998).
[14] K. Nowinska, A. Waclaw, W. Masierak, A. Gutsze. *Catal. Lett.*, **92**, 157 (2004).
[15] M.S.S. Balula, I. Santos, J.A.F. Gamelas, A.M.V. Cavaleiro, N. Binsted, W. Schlindwein. *Eur. J. Inorg. Chem.*, 1027 (2007).
[16] X. Zhang, M.T. Pope, M.R. Chance, G.B. Jameson. *Polyhedron*, **14**, 1381 (1995).
[17] C.L. Hill, C.M. Prosser-McCartha. *Coord. Chem. Rev.*, **143**, 407 (1995).
[18] T.J.R. Weakley, S.A. Malik. *J. Inorg. Nucl. Chem.*, **29**, 2935 (1967).
[19] D.E. Katsoulis, M.T. Pope. *J. Am. Chem. Soc.*, **106**, 2737 (1984).
[20] D.E. Katsoulis, M.T. Pope. *J. Chem. Soc., Chem. Commun.*, 1186 (1986).
[21] D.E. Katsoulis, M.T. Pope. *J. Chem. Soc., Dalton Trans.*, 1483 (1989).
[22] L.A. Combs-Walker, C.L. Hill. *Inorg. Chem.*, **30**, 4016 (1991).
[23] X. Lin, G. Gao, L. Xu, F. Li, L. Liu, N. Jiang, Y. Yang. *Solid State Sci.*, **11**, 1433 (2009).
[24] T. Mazari, C.R. Marchal, S. Hocine, N. Salhi, C. Rabia. *J. Nat. Gas Chem.*, **18**, 319 (2009).
[25] E. Coronado, J.R. Galán-Mascarós, C. Giménez-Saiz, C.J. Gómez-García, S. Triki. *J. Am. Chem. Soc.*, **120**, 4671 (1998).
[26] J. Hu, R.C. Burns. *J. Mol. Catal. A: Chem.*, **184**, 451 (2002).

[27] Bruker. *SADABS, SMART, SAINT and SHELXTL*, Bruker AXS Inc., Madison, WI, USA (2000).
[28] G.M. Sheldrick. *SHELX-97, Program for Crystal Structure Solution and Analysis*, University of Gottingen, Gottingen, Germany (1997).
[29] A. Vogel. *A Textbook of Quantitative Inorganic Analysis*, 2nd Edn, Longmans, Green and Co., London (1951).
[30] T.J.R. Weakly. *J. Crystall. Spec. Res.*, **17**, 383 (1987).
[31] R.F. Klevtsova, E.N. Yarchenko, L.A. Glinskaya, L.I. Kuznetsova, L.G. Detusheva, T.P. Lazarenko. *Zh. Strukt. Khim.*, **32**, 102 (1991).
[32] M. Sadakane, D. Tuskuma, M.H. Dickman, U. Kortz, M. Higashijima, W. Ueda. *Dalton Trans.*, 4271 (2006).